Biointerface Research in Applied Chemistry
Platinum Open Access Journal (ISSN: 2069-5837)

Article
Volume 11, Issue 1, 2021, 8171 - 8178
https://doi.org/10.33263/BRIAC111.81718178

Efficient Blue Luminescent Graphene Quantum Dots and their Photocatalytic Ability Under Visible Light

Peetam Mandal [1], Kandarpa Kumar Nath [1], Mitali Saha [1,*]

[1] Department of Chemistry, National Institute of Technology Agartala, Tripura – 799046, India
* Correspondence: mitalichem71@gmail.com;

Scopus Author ID 55779373600

Received: 14.06.2020; Revised: 16.07.2020; Accepted: 17.07.2020; Published: 19.07.2020

Abstract: Graphene Quantum Dots (GQDs) are considered to be a new class of materials with distinctive photoluminescence and low toxic level properties. Herein, we have reported the preparation of GQDs at different pH (pH 5, 8, 10, and 14) from pyrocatechol. UV-Visible absorption and normalized fluorescence spectra were applied to analyze the optical properties of GQDs at different pH. DLS and AFM had been performed to study the mean particle size and the morphology of the GQDs. Further, the photocatalytic behavior of the synthesized GQDs obtained at pH 10 was used in the degradation of dyes viz. Methylene Blue and Methyl Orange under visible-light irradiation. The influence of certain parameters such as pH of the GQD, contact time, a dosage of GQDs, and the kinetic model was demonstrated. The plausible mechanism of degradation of the toxic dyes based on GQDs under visible light illumination was discussed, too.

Keywords: GQD; dye degradation; photocatalysis; Methylene Blue; Methyl Orange; photodegradation.

1. Introduction

Dyes are a prime coloring agent in textile industries and also have multiple applications viz. food additives, tanning, MRI imaging, etc. Fifteen percent of dyes are unwantedly dispatched into surrounding water bodies during its production [1], leading to multiple cases of mutagenic destruction in the biological food web system both directly and indirectly [2]. Unlike other organic compounds, their high solubility in aqueous as well as organic solvents makes them severely challenging to separate and degrade it under conventional wastewater and sludge treatment process [3]. These dyes are highly responsible for the contamination of ground and surface water, causing carcinogenic diseases among living organisms [4].

The rise of nanotechnology and its application in water treatment had been a boon, and a large number of metal nanoparticles (NPs) were used in decolorizing the toxic effluent dyes [5, 6]. CdS [7], CuO [8], Fe_2O_3 [9], ZnO [10], V_2O_5 [11], Au_2O_3 [12], Ag_2O [13] are some of the commonly used metal NPs in photocatalytic dye degradation. The semiconducting metal oxides have ample bandgap to catalyze the photochemical degradation process, but most of them have demerit of being carcinogenic [14]. It is well known that nano metal oxides doesn't solubilize in water either have proper dispersion in any solvent. Therefore a large amount of these metal nanoparticles after several photocatalytic cycles are considered to be depleted leftover. Although these metal NPs have the efficiency to work as photocatalyst, their lethal effect on the living organisms can't be underestimated [15]. The synthesis of these metal

nanoparticles either requires high thermal energy, hydrothermal conditions, and controlled chemical vapor deposition process, or their precursors are very expensive [16]. Graphene Quantum Dots (GQD) emerged as a significant bio-compatible zero-dimensional substance with its multiple usages in drug delivery [17], photovoltaics [18], electrochemical sensing [19], bio-imaging [20], gene delivery [21], anti-cancer drugs [22] yet photocatalytic degradation of dyes are exceedingly limited. In continuation of our previous synthesis works with the synthesis of graphene oxide, graphene and GQDs [23-26], this paper aimed to develop GQDs for the first time from pyrocatechol at 100^{o} C. The synthesized GQDs have shown excellent photocatalytic activity against the degradation of two toxic dyes, i.e., Methylene Blue and Methyl Orange. These economical and energetically favorable synthesized GQDs in a mere two hours can prove to be a promising candidate for the toxic dye scavenging.

2. Materials and Methods

2.1. Material characterization.

The absorption spectra of the GQDs and the dyes were obtained by Shimadzu 1800 UV–Vis spectrophotometer in the range of 190–800 nm. The steady-state photoluminescence spectra were measured using fluorescence Perkin Elmer LS 55 fluorescence spectrometer. The particle size distributions of the GQDs formed were obtained at four different pH viz. pH 5, 8, 10 and 14 using Nanotrac wave W3222 dynamic light scattering (DLS) at 25^{o} C. Atomic Force Microscopy (AFM) was done in Bruker MultiMode V8 to investigate the morphology of the products on a glass substrate at room temperature.

2.2. Synthesis of graphene quantum dots GQDs.

In a typical synthesis process, a suspension of 3 gm Pyrocatechol crystals (Astron Chemicals, India, analytical reagent grade) was heated around its melting range (100-105^{o} C) for 45 minutes. The ash - grey powder was transformed into pale black syrupy liquid upon heat treatment. The molten liquid was kept for prolonging heating at a reduced temperature around 60^{o} C for an hour. The syrupy liquid was cooled to room temperature prior to further preparation procedure. 0.5 M standard sodium hydroxide (Merck Life Science Pvt. Ltd, EMPLURA® grade) solution was prepared and injected dropwise on the molten brownish resultant to adjust and obtain various independent pH. Collectively, four samples of different pH at 5, 8, 10, 14 samples were prepared. The resultant brownish colored liquids were found to be highly soluble in water.

2.3. Photochemical experimental setup.

The entire photocatalytic degradation of Methylene Blue and Methyl Orange was carried out on a stirrer under commercial 40 W CFL lamp (Oreva) illuminations at room temperature. 5 mg of Methyl Orange powder (Alfa Aesar®) was added in 500 ml of de-ionized water and was fourfold diluted to make a dye solution of 1.909 x 10^{-6} mol/L. Similarly, the solution of Methylene Blue (Merck Millipore™, Reag. Ph Eur. Grade) was freshly prepared with a molar concentration of around 1.954 x 10^{-6} mol/L. 40 ml of dye solutions were taken from the stock solutions in separate beakers, and 10 ml of the synthesized photocatalyst was added to it. The solutions were stirred under the CFL lamp, and after an interval of every 30 minutes (until 120-minute spans), 5 ml of the dye solution was collected through a disposable

syringe filter and stored for absorbance studies in UV – Vis spectrophotometer. The steady kinetics of the reaction was briefly explained. The entire reaction process was done under a rapid span of 120 minutes, and a comparative study was done among the photocatalytic degradation of the three dyes, illustrating the role of the facile GQDs in photocatalytic degradation.

3. Results and Discussion

The synthesis of GQD was performed upon heating pyrocatechol at around its melting point (100 – 105^{o} C) for a span of 45 minutes, and color change was observed from ash-grey powder to pale black syrupy liquid. GQDs at different pH were prepared upon addition of 0.5 M sodium hydroxide solution, and all the different samples of GQDs at pH 5, 8 10, and 14 were highly soluble in an aqueous medium. The GQDs at all different pH showed a typical sharp absorption peak in the ultraviolet region at 264 nm with a tail extending to the visible range, as shown in Figure 1a. It may be attributed to some absorption shoulders for the π–π* transition of the C=C bonds, n–π* transition of C=O bonds and/or others. The UV–Vis spectra clearly indicated that on decreasing the pH, the absorption peaks become less intense, which suggested the increase of distribution of particle sizes with the decrease of pH. At pH 10, the intensity of the absorption peak was found to be maximum, which further decreased at pH 14.

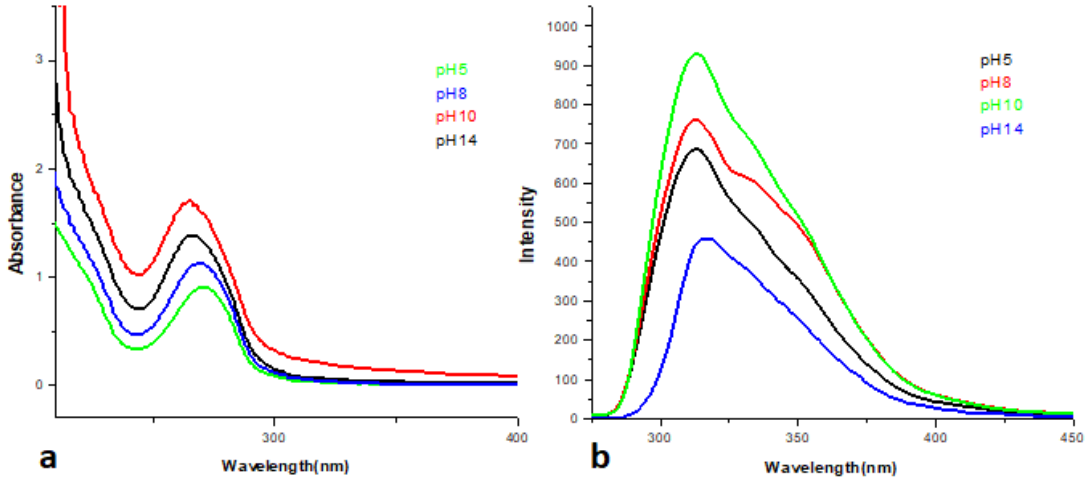

Figure 1. (a,b) UV-visible spectra and fluorescence spectra of GQD$_S$ at different pH, respectively.

Similarly, in Figure 1b, the fluorescence spectra were recorded for various pH oriented GQDs. A strong peak in the fluorescence emission spectrum was recorded with maxima at 316 nm. Fluorescence spectra exhibited that the intensity of the peak was found to be more at pH 10 as compared to another pH. However, the intensity of the peak declined at pH 14. The particle size distributions of the GQDs were carried out at 25 °C using dynamic light scattering (DLS) at varying pH in Figure 2. It was found that at pH 5, the average particle size was around 1 nm, and the yield was 94%. In the case of pH 8, 70% of the GQDs were found to be around 0.9 nm in size. On further increasing the pH up to 10 of the solution, the yield of the nanoparticles increases up to 83%, increasing the average particle size ~ 8 nm only. At pH 14, 75% of the particles had an average particle size of 4 nm. It may be attributed to the fact that in case of lower pH, the presence of hydroxyl groups hindered the aggregation of the nanoparticles. But on increasing the pH, the increasing number of hydroxyl groups gets adhered

to the nanoparticles and hence increased the size of the nanoparticles. At pH 10 the average particle size was greater, which indicated more aggregation of the carbon nanoparticles. Thus, the pH of the solutions played an important role in the synthesis of GQDs with a size below 10 nm.

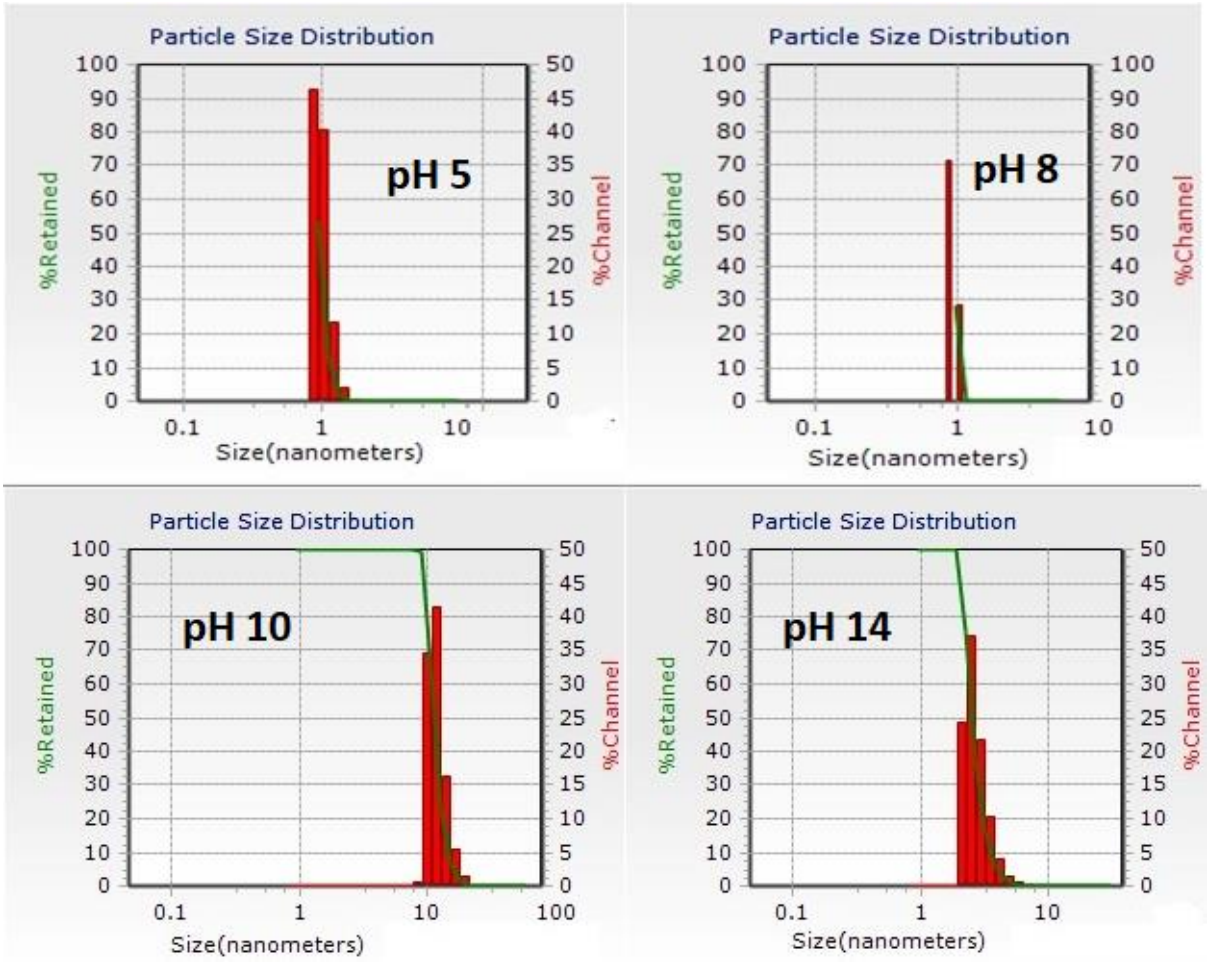

Figure 2. Average particle size distribution histograms of GQDs at different pH.

In Figure 3, AFM showed the topographic images of well-dispersed GQDs at various pH. The AFM images confirmed the formation of spherical-shaped GQDs, where the particle sizes were below 10 nm in pH 10 (Figure 3c). The image clearly depicted that at alkaline pH 10 it was having uniform spherical shape whereas in case of pH 5 (Figure 3a) the spherical GQDs agglomerated with one another to obtain the larger shape. It might be attributed that in acidic medium, the particles get hindered by the proton-rich environment to retain smaller shapes as quantum dots are highly reactive. Similarly, extreme alkalinity, i.e., pH 14, was not ideal to have particle shape confined within the 10 nm range and had formed larger particles (Figure 3d). Thus alkalinity was found to be the ideal condition to form GQDs.

Photocatalytic activity of the synthesized GQDs was studied in the degradation of two dyes viz. methylene blue and methyl orange. Figure 4 showed the trend of gradual structural decomposition of the two dyes, which was monitored by observing the color change at regular time intervals up to 120 mins. Figure 4a showed that the absorption peaks at 543 nm for methylene blue were decreased gradually with the increase of the exposure time, which indicated the photocatalytic degradation reaction of methylene blue. As shown in Figure 4, the degradation of methylene blue had started within 30 mins and completed almost after 120 mins. Figure 4b showed that methyl orange is an azoic dye that resisted the degradation up to 60 min but degraded completely within 120 min. Therefore, it can be concluded that the synthesized

GQDs has the capability to degrade these two organic dyes and can be potentially used for the degradation of other organic dyes and pollutants. In two hours, Methyl Orange had decolorized to 52 percent but the mineralized product formation from Methylene Blue, around 79.4 percent (Figure 4c & d). Thus the degradation of Methylene Blue was higher than Methyl Orange.

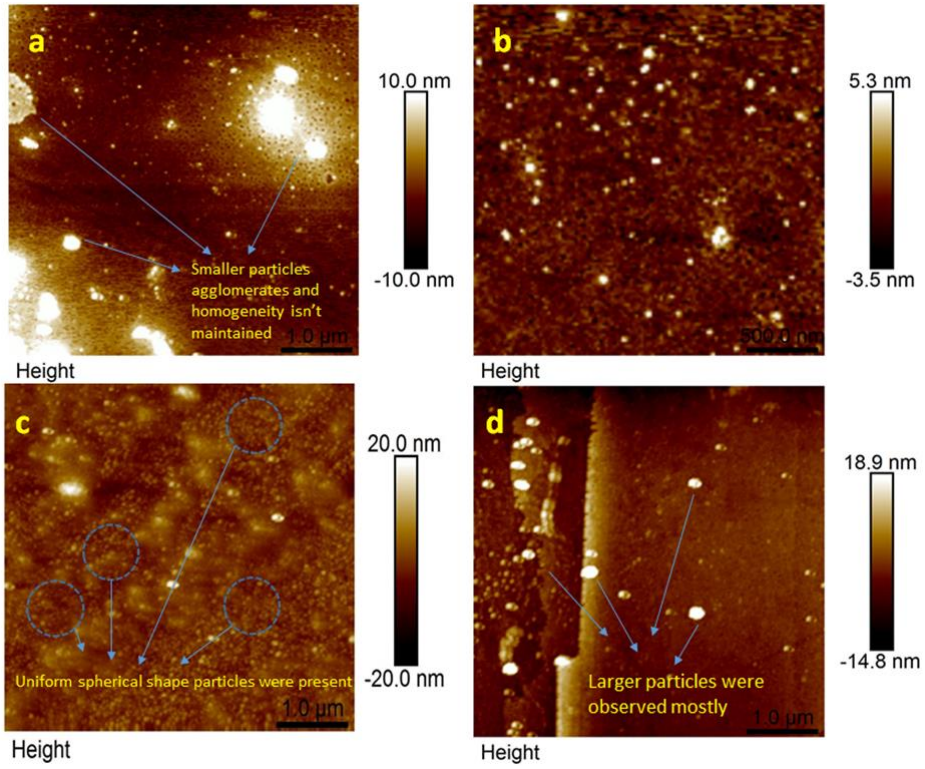

Figure 3. AFM images of GQDs at various pH (a) pH 5 (b) pH 8 (c) pH 10 and (d) pH 14.

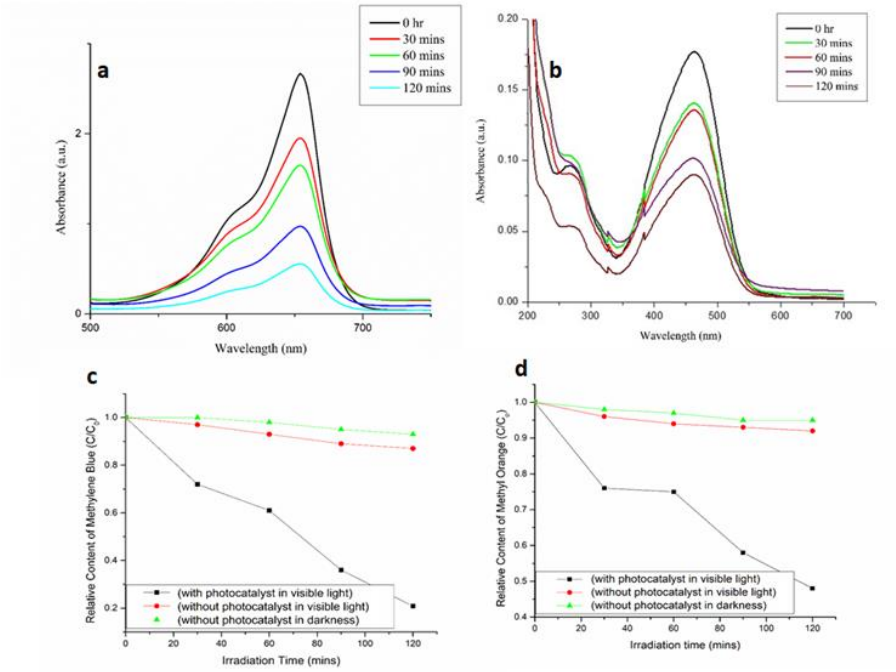

Figure 4. Absorbance spectra of (a) Methylene Blue and (b) Methyl Orange. The relative content of (c) Methylene Blue and (d) Methyl Orange during the photocatalytic degradation process.

The Langmuir – Hinshelwood model was applied on the kinetics of Methyl Orange and Methylene Blue degradation over the entire experiment on visible light exposure as shown by

$$\log (C_o/C) = kt$$

Here, k is the pseudo-first-order rate constant as the concentration of the solvent is in excess to that of the dye. The plot log (C_o/C) versus irradiation time (where C_o is the initial concentration of the dye and C is the concentration of the dye in the reaction time) was found out to be linear as shown in Figure 5, which suggested that photodegradation reactions followed pseudo-first-order kinetics. The apparent reaction rate constant (k) for Methylene Blue and Methyl Orange was found to be 0.01133 min^{-1} and 0.00519 min^{-1}, respectively. The decreasing order of the rate constants followed the order- Methylene Blue > Methyl Orange, which was found to be consistent with the photocatalytic degradation results presented in (C/C_o) versus irradiation time (min) graph. In Figure 5, the pseudo-first-order kinetics had been shown, with straight lines stretched to depict the k value.

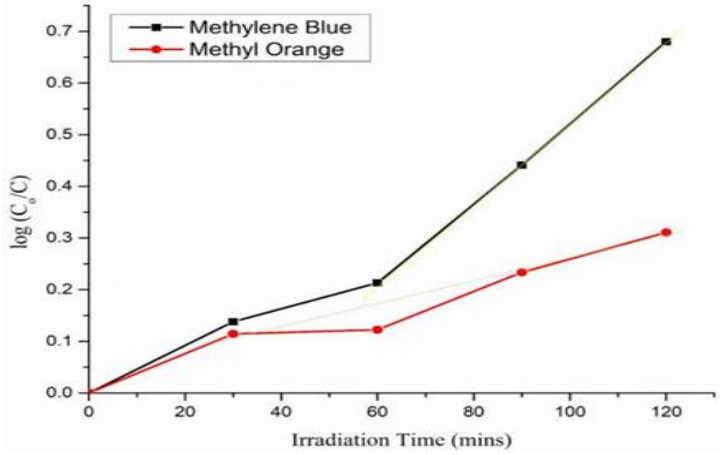

Figure 5. Pseudo 1st order kinetics of the two dyes photo-catalyzed by GQDs.

In Figure 6, a plausible mechanism of the photocatalysis of the two dyes undergoing on the surface of GQDs had been illustrated. In photocatalytic degradation of the organic dyes, the following steps might took place: surface adsorption of the dyes which was directly proportional to the surface area and dispersion of the photocatalyst; the adsorption of visible light by the dye, which promoted the dye to the excited state; the transfer of an electron from the excited state to the conductive band of the photocatalyst and consequently the formation of effective radicals from water or oxygen and the oxidation of the dye by the radicals.

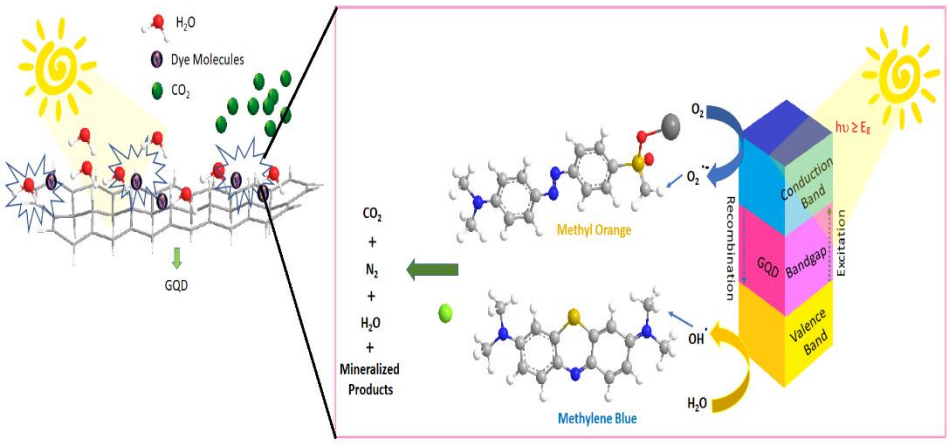

Figure 6. Plausible mechanism of the photocatalysis undergoing on the surface of the GQDs.

The results showed that the GQDs, synthesized from heat treatment was effective in the photocatalytic degradation of these two dyes. Therefore, it can be concluded that the synthesized GQDs has the capability to degrade these two organic dyes and can be potentially used for the degradation of other organic dyes and pollutants. In addition, GQD photocatalysis may be envisaged as a method for the treatment of diluted wastewaters in the textile industries.

4. Conclusions

The synthesis of GQDs from pyrocatechol was highly successful, and thus, DLS and AFM studies proved that GQDs at pH 10 had homogenous spherical shape at a size of ~ 8 nm. The absorbance spectra were taken for both the dyes after the degradation process continued for various time intervals and showed that Methyl Orange degraded to 52 % while Methylene Blue degraded 79.4 % within two hours. The reaction rate constant (k) for Methyl Orange and Methylene Blue was found to be 0.00519 min^{-1} and 0.01133 min^{-1}, respectively.

Funding

This research received no external funding.

Acknowledgments

The authors like to thank the Department of Chemistry for DLS, UV-Visible and Fluorescence spectra, and the Central Research Facility (CRF) of NIT, Agartala for the Atomic Force Microscopy (AFM) images.

Conflicts of Interest

The authors declare no conflict of interest.

References

1. Sangon, S.; Hunt, A.J.; Attard, T.M.; Mengchang, P.; Ngernyen, Y.; Supanchaiyamat, N. Valorisation of waste rice straw for the production of highly effective carbon based adsorbents for dyes removal. *J. Clean. Prod.* **2018**, *172*, 1128-1139, https://doi.org/10.1016/j.jclepro.2017.10.210.
2. Sponza, D.T. Toxicity studies in a chemical dye production industry in Turkey. *J. Hazard. Mater*. **2006,** *138*, 438-447, https://doi.org/10.1016/j.jhazmat.2006.05.120.
3. Tichonovas, M.; Krugly, E.; Racys, V.; Hippler, R.; Kauneliene, V.; Stasiulaitiene, I.; Martuzevicius, D. Degradation of various textile dyes as wastewater pollutants under dielectric barrier discharge plasma treatment. *Chem. Eng. J.* **2013,** *229*, 9-19, https://doi.org/10.1016/j.cej.2013.05.095.
4. de Oliveira, G.A.R.; Leme, D.M.; de Lapuente, J.; Brito, L.B.; Porredón, C.; de Brito Rodrigues, L.; Brull, N.; Serret, J.T.; Borràs, M.; Disner, G.R.; Cestari, M.M. A test battery for assessing the ecotoxic effects of textile dyes. *Chem. Biol. Interact.* **2018**, *291*, 171-179, https://doi.org/10.1016/j.cbi.2018.06.026.
5. Ma, J.; Liu, C.; Chen, K. Removal of Cr (VI) species from water with a newly-designed adsorptive treatment train. *Sep. Purif. Technol.***2020,** *234*, https://doi.org/10.1016/j.seppur.2019.116041.
6. Mulchandani, A.; Atkinson, A.J.; Garcia-Segura, S.; Westerhoff, P. "Nanoblocks": A Playful Method To Learn about Nanotechnology-Enabled Water and Air Treatment. *J. Chem. Educ*. **2019,** *96*, 708-713, https://doi.org/10.1021/acs.jchemed.8b00535.
7. Saha, M.; Ghosh, S.; De, S.K. Nanoscale Kirkendall Effect Driven Au Decorated CdS/CdO Colloidal Nanocomposites for Efficient Hydrogen Evolution, Photocatalytic Dye Degradation and Cr (VI) Reduction. *Catal. Today* **2020,** *340*, 253-267, https://doi.org/10.1016/j.cattod.2018.11.027.
8. Narasaiah, B.P.; Mandal, B.K. Bio-fabricated CuO NPs as green catalyst towards remediation of environmental pollutants. *Lett. Appl. NanoBioScience*, **2019,** *8*, 597-603. https://doi.org/10.33263/LIANBS83.597603.
9. Pouran, S.R.; Bayrami, A.; Shafeeyan, M.S.; Raman, A.A.A.; Daud, W.M.A.W. A comparative study on a cationic dye removal through homogeneous and heterogeneous Fenton oxidation systems. *Acta Chim. Slov.* **2018,** *65*, 166-171, http://dx.doi.org/10.17344/acsi.2017.3732.

10. Habtemariam, A.B.; Sibhatu, A.K.; Weldegebrieal, G.K.; Zelekew, O.A.; Tekletsadik, B.T. Bio-mediated synthesis of ZnO nanostructures from Thymus Schimperi leaves extract and its antibacterial and photocatalytic activities. *Lett. Appl. NanoBioScience*, **2020**, *9*, 808-813. https://doi.org/10.33263/LIANBS91.808813.
11. Jayaraman, V.; Sarkar, D.; Rajendran, R.; Palanivel, B.; Ayappan, C.; Chellamuthu, M.; Mani, A. Synergistic effect of band edge potentials on BiFeO3/V2O5 composite: Enhanced photo catalytic activity. *J. Environ. Manage.* **2019,** *247*, 104-114, https://doi.org/10.1016/j.jenvman.2019.06.041.
12. Nadaf, N.Y.; Kanase, S.S. Biosynthesis of gold nanoparticles by Bacillus marisflavi and its potential in catalytic dye degradation. *Arab. J. Chem.* **2019,** *12*,4806-4814, https://doi.org/10.1016/j.arabjc.2016.09.020.
13. Akhondi, M.; Jamalizadeh, E. Fabrication of silver-modified halloysite nanotubes and their catalytic performance in rhodamine 6G and methyl orange reduction. *Acta Chim.Slov.***2019**, *66*, 136-144, http://dx.doi.org/10.17344/acsi.2018.4726.
14. Lekamge, S.; Ball, A.S.; Shukla, R.; Nugegoda, D. The toxicity of nanoparticles to organisms in freshwater. *Rev. Environ. Contam. T.* **2020,** *248*, 1-80, https://doi.org/10.1007/398_2018_18.
15. Wang, L.; Yang, D.; Li, Z.; Fu, Y.; Liu, X.; Brookes, P.C.; Xu, J. A comprehensive mitigation strategy for heavy metal contamination of farmland around mining areas–Screening of low accumulated cultivars, soil remediation and risk assessment. *Environ. Pollut.* **2019**, *245*, 820-828, https://doi.org/10.1016/j.envpol.2018.11.062.
16. Zhang, Q.; Zhang, L.; Wu, W.; Xiao, H. Methods and applications of nanocellulose loaded with inorganic nanomaterials: A review. *Carbohyd. Polym.* **2020**, *229*, https://doi.org/10.1016/j.carbpol.2019.115454.
17. Vatanparast, M.; Shariatinia, Z. Revealing the role of different nitrogen functionalities in the drug delivery performance of graphene quantum dots: a combined density functional theory and molecular dynamics approach. *J. Mater.Chem. B*, **2019,** *7*, 6156-6171, https://doi.org/10.1039/C9TB00971J.
18. Gebreegziabher, G.G.; Asemahegne, A.S.; Ayele, D.W.; Mani, D.; Narzary, R.; Sahu, P.P.; Kumar, A. Polyaniline–graphene quantum dots (PANI–GQDs) hybrid for plastic solar cell. *Carbon Lett.* **2020,** *30*, 1-11, https://doi.org/10.1007/s42823-019-00064-6.
19. Anh, N.T.N.; Chang, P.Y.; Doong, R.A. Sulfur-doped graphene quantum dot-based paper sensor for highly sensitive and selective detection of 4-nitrophenol in contaminated water and wastewater. *RSC Adv.* **2019,** *9*, 26588-26597, https://doi.org/10.1039/c9ra04414k.
20. Lu, H.; Li, W.; Dong, H.; Wei, M. Graphene quantum dots for optical bioimaging. *Small* **2019**, *15*, https://doi.org/10.1002/smll.201902136.
21. Taghavi, S.; Abnous, K.; Taghdisi, S.M.; Ramezani, M.; Alibolandi, M. Hybrid carbon-based materials for gene delivery in cancer therapy. *J. Control. Release* **2020,** *318*, 158-175, https://doi.org/10.1016/j.jconrel.2019.12.030.
22. De, S.; Patra, K.; Ghosh, D.; Dutta, K.; Dey, A.; Sarkar, G.; Maiti, J.; Basu, A.; Rana, D.; Chattopadhyay, D. Tailoring the efficacy of multifunctional biopolymeric graphene oxide quantum dot-based nanomaterial as nanocargo in cancer therapeutic application. *ACS Biomater. Sci. Eng.* **2018**, *4*, 514-531, https://doi.org/10.1021/acsbiomaterials.7b00689.
23. Mandal, P.; Debbarma, J.; Saha, M. One Step Synthesis of N-Containing Graphene Oxide from 3-Aminophenol. *Cryst. Res. Technol.***2020**, *55*, https://doi.org/10.1002/crat.201900158.
24. Mandal, P.; Saha, M. Low-temperature synthesis of graphene derivatives: mechanism and characterization. *Chem. Pap.* **2019**, *73*, 1997-2006, https://doi.org/10.1007/s11696-019-00756-3.
25. Mandal, P.; Naik, M.J.P.; Saha, M. Room temperature synthesis of graphene nanosheets. *Cryst. Res. Technol.* **2018**, *53*, https://doi.org/10.1002/crat.201700250.
26. Naik, M.J.P.; Mohanta, S.; Mandal, P.; Saha, M. N-Doped Graphene Quantum Dots Using Different Bases. *Int. J. Nanosci.* **2019**, *18*, https://doi.org/10.1142/S0219581X18500175.